

## The mechanical properties of a silicon nanowire under uniaxial tension and compression

Chi Yan Tang<sup>1</sup>, L.C. Zhang<sup>1</sup> and Kausala Mylvaganam<sup>1</sup>

<sup>1</sup>School of Aerospace, Mechanical and Mechatronic Engineering, University of Sydney, NSW 2006, Australia

**Abstract:** This paper studies the mechanical properties of a silicon nanowire (SiNW) under uniaxial tension and compression with the aid of the molecular dynamics method. The three-bodied Tersoff potential is used to describe the silicon atomic interactions. It was found that under tension, SiNW exhibits rapid necking followed by a continuous unravelling of amorphous silicon atoms featuring a chain of single atoms. During compressive loading, the SiNW undergoes a large post-buckling deflection in its elastic regime. Irreversible deformation via amorphization only occurs in six localized zones before fracture.

**Keywords:** Silicon nanowire, molecular simulation, mechanical properties, uniaxial tension, uniaxial compression

### 1 Introduction

One-dimensional nanostructures such as silicon nanowires (SiNWs) have attracted extensive research attention due to its importance to a wide variety of nano-electromechanical (NEM) applications. A SiNW is a rod consisting of thousands of atoms with a cross-sectional dimension of nanometer scale and can be used as a fundamental building block for nano-electronic devices such as high-performance field-effect transistors [1-3]. Cui *et al* suggests that the performance of SiNWs could potentially surpass that of conventional devices. Nanowires can also be used as highly sensitive, real-time electrically based sensors for biological and chemical species [4].

Recent studies on SiNWs have focused on the synthesis and fabrication techniques. SiNWs are conventionally synthesized by chemical vapour deposition (CVD) via the vapour-liquid-solid (VLS) mechanisms where monosilane ( $\text{SiH}_4$ ) is used with gold serving as a catalyst to facilitate growth [5-7]. Only a narrow set of conditions of chemical concentration and temperature can yield highly controllable growth of aligned nanowires [5]. It was found that with the aid of transmission electron microscopy (TEM), SiNWs with smaller diameters grow slower, and that a critical diameter at which growth stops completely does exist [6]. More recently, SiNWs have also been synthesized via field emission [8], laser ablation and thermal evaporation methods [9].

Little investigation has been conducted on the nano-mechanical properties of SiNWs [10-13]. Apart from the technical difficulties in conducting nano-mechanical tests, the interpretation of results arising from the use of these methods in order to understand such mechanical behaviour and material characteristics is frequently impeded by ambiguities. Thus on this scale, molecular dynamics analysis is an ideal tool to examine the precise nature of the atomic bonding and mechanical transformations of strain-induced fracture and amorphization. A study of molecular potentials indicates that the Tersoff potential is suitable to represent the reconstruction of a nanowire surface [12]. A recent work based on non-orthogonal tight-binding molecular dynamics methods [13] indicate that SiNWs are composed of a crystalline core surrounded by a bond distorted-dominated region and that a critical diameter below which a crystalline nanowire becomes unstable exists due to surface-surface interaction. The present study will investigate the mechanical properties of a SiNW under uniaxial tension and compression with the aid of the three-bodied Tersoff potential.

## 2 Modelling

The model of a SiNW used in the simulations has a hexagonal profile with four  $\langle 111 \rangle$  sides, two  $\langle 100 \rangle$  sides and a length of 301.4 Å. The SiNW's cross-section is in the  $\langle 110 \rangle$  plane with an average radius of 11.7 Å. This length is sufficiently long for minimizing the boundary effects. The silicon atoms are assumed to be chemically inert and that the deformations of the SiNW take place in a vacuum environment. Figure 1 displays the initial model of the SiNW in the crystalline state.

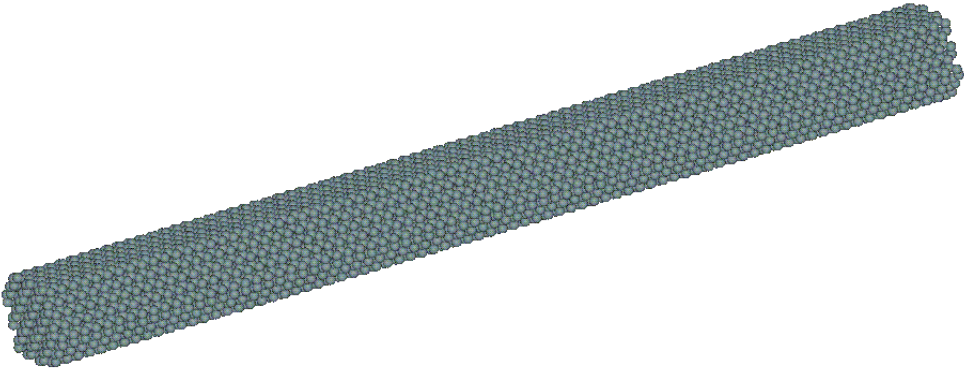


Figure 1. Initial model of the silicon nanowire.

As the directionality of the silicon bonding is important, the three-bodied Tersoff potential is used [14]. This empirical potential has been demonstrated to be reliable [12, 15] and can be used to adequately predict the covalent bonding of crystalline and amorphous phases of silicon. The steepest descent method is used to iteratively minimize the total energy of the system so that the structure of silicon nanowire is energetically optimized. The algorithm is given by:

$$x_0 - x_1 = \alpha \left( \frac{dV}{dX} \right) \quad (1)$$

where  $x_0$  and  $x_1$  represent the positions of atoms at different iterative steps,  $\alpha$  is a small enough positive number and  $dV/dX$  is the energy gradient of the system.

Based on this, the positions of inner silicon atoms of the nanowire atoms show negligible change in position while the radius of the SiNW drops by 0.83% as a result of the shrinkage of energetically unfavourable lesser-coordinated outer layer atoms. A related study on the annealing and relaxation of a SiNW over thousand of timesteps shows similar results [12]. The shrinkage along the axial direction has been shown to be negligible.

The SiNW model consists of a total of 8630 atoms with two layers on both ends of the wire held rigidly. The classical Verlet integrator is used with a simulation timestep of 2.5 fs. The uniaxial strain rate is  $3.53 \times 10^8 \text{ s}^{-1}$  and is applied by means of simultaneously pulling the fixed atoms of both ends of the SiNW. This energetically optimized structure is relaxed for a further thousand timesteps before tension or compression is applied. During the simulations, the average temperature of all atoms is held constant at 293° K by scaling their velocities at every timestep.

### 3 Results and discussion

#### 3.1 Tension

The SiNW deforms elastically with a uniform increase in the distances between the silicon layers along the axial directions. The SiNW starts to undergo irreversible plastic deformation at strain  $\epsilon=33.2\%$  with necking occurring in two zones near the ends as shown in Figure 2(a). The crystalline order in the zone rapidly deteriorates into an amorphous phase as shown in Figure 2(b). This region rapidly thins down and the amorphous zone develops into a single-layered Si-Si atomic chain. On the application of further tension, the atomic chain grows longer (Figure 2(c)) due to an unravelling of amorphous silicon from the shrunk amorphous regions. This phenomenon has also been noted in a molecular dynamics simulation study of tensile loading of carbon nanotubes using the Tersoff-Brenner potential [16]. No shear banding of the SiNW was observed.

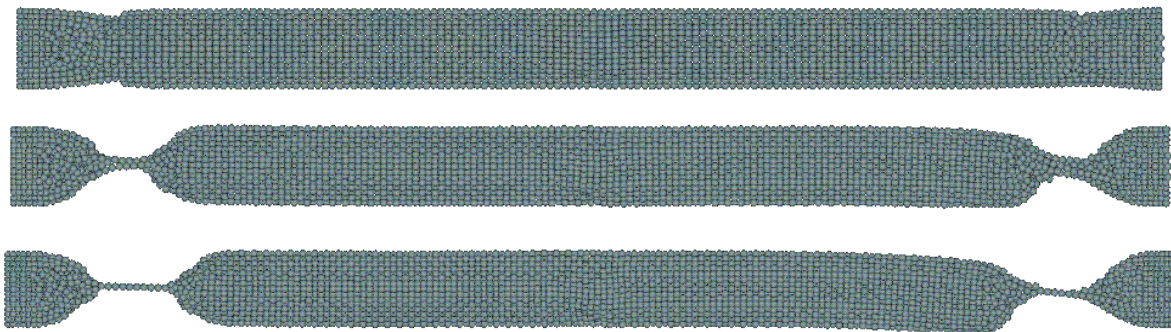


Figure 2. Atomic chain of a SiNW under uniaxial tension. The displayed nanowires occur at (a) 110000 timesteps ( $\epsilon=33.2\%$ ), (b) 128000 timesteps ( $\epsilon=39.2\%$ ), (c) 155000 timesteps ( $\epsilon=48.1\%$ ).

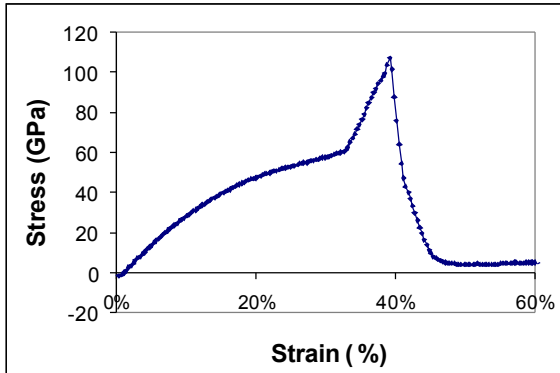


Figure 3. Stress-strain relationship of the SiNW under tension.

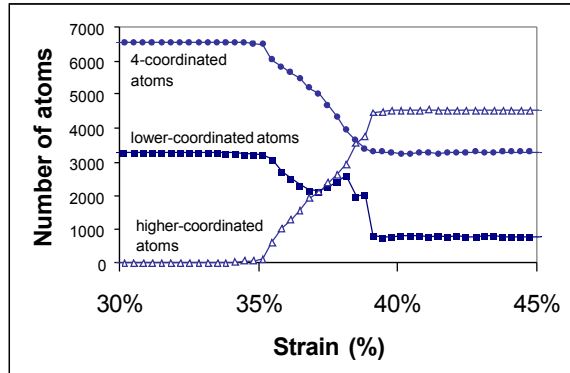


Figure 4. Number of atoms with specified nearest number of neighbouring atoms against tensile strain.

Figure 3 displays the stress-strain relationship for a SiNW under uniaxial tension. The stresses are derived from averaging the total atomic forces of the individual atoms along both tips of the SiNW. The Young's Modulus obtained from the slope of the stress-strain curve in the elastic region is calculated to be 352.0 GPa, which is higher than the values reported in literature [17] due to scale effects that arise from surface-surface interactions.

A view of the coordination states of the silicon atoms in the nanowire can provide information on the crystalline-to-amorphous microstructure changes that occur during tension. Fourfold-coordinated atoms generally indicate the number of crystalline silicon atoms while the higher coordinated atoms indicate the number of amorphous silicon atoms. From  $\epsilon=0\%$  to  $\epsilon=33.2\%$ , the nanowire does not exhibit any changes from the original crystalline structure with all the inner layer atoms remaining as

fourfold-coordinated atoms. As the structure starts to yield at  $e=33.2\%$ , zones of multi-coordinated atoms form which indicates that the crystalline lattice structure is disintegrating. An earlier study has also shown that the strain rate can also induce amorphization in homogenous elastically strained face-centered-cubic (FCC) single crystal metallic nanowires [18].

### 3.2 Compression

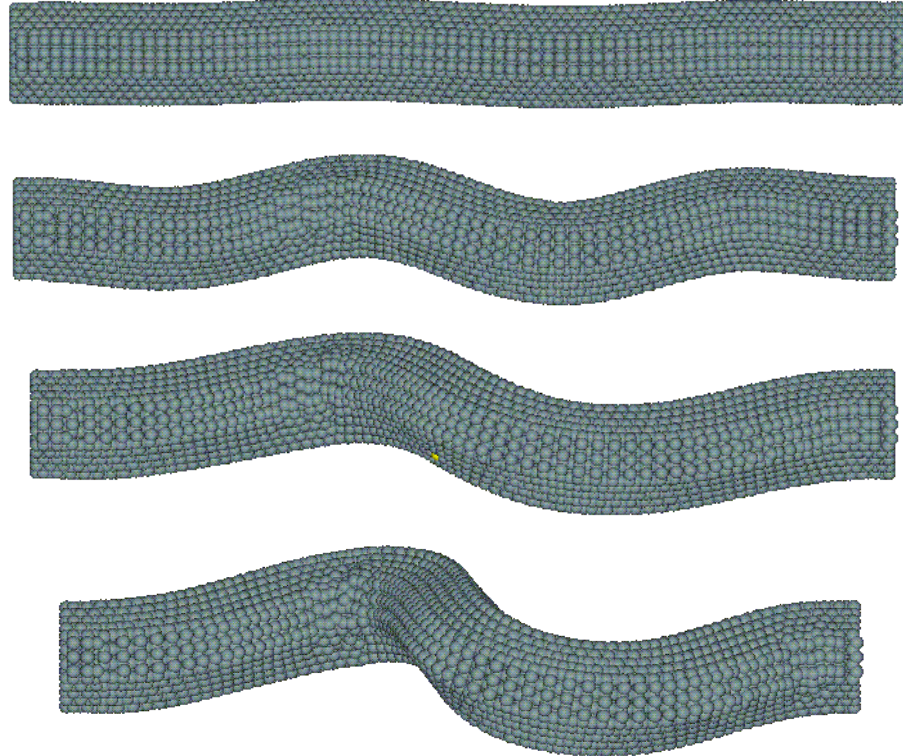


Figure 5. SiNW under uniaxial compression. The displayed nanowires occur at  
 (a) 45000 timesteps ( $e=-11.6\%$ ), (b) 53000 timesteps ( $e=-14.3\%$ ), (c) 71000 timesteps ( $e=-20.2\%$ ),  
 (d) 100000 timesteps ( $e=-29.9\%$ ).

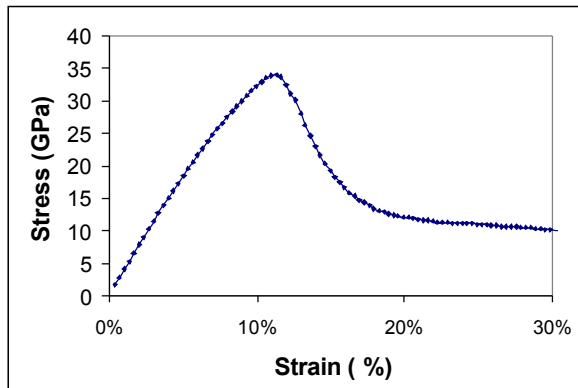


Figure 6. Stress-strain relationship of the SiNW under tension.

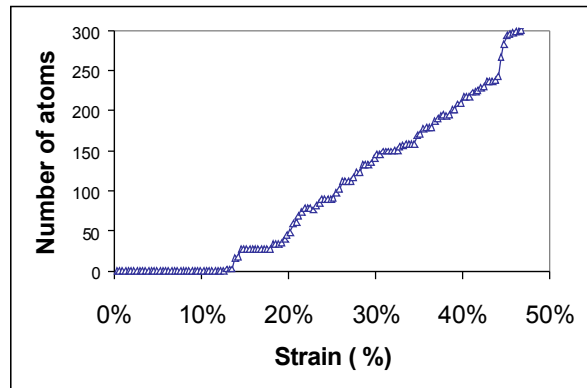


Figure 7. Number of high-density amorphous atoms against compressive strain.

Figure 5 displays the cross-sectional views of a SiNW under constant compressive loading while Figure 6 displays the stress-strain relationship of a SiNW under compression. The SiNW initially undergoes elastic deformation indicated by the linear stress-strain relationship in Figure 6 which can be characterized primarily with a decrease of bond distances along the axial direction. The onset of buckling and plastic deformation occurs at  $e=-10.9\%$ , while higher-coordinated atoms start to form at the two compressed zones at  $e=-14.9\%$  as indicated in Figure 7. This region is indicated with the

dashed circles in Figure 8. The amorphization in these regions is due to high compressive stresses. In conventional continuum mechanics, it is well established that long bars will buckle under an axial compression when the load reaches the critical buckling point [19], and that phenomenon is similar to this SiNW. The size of these amorphous regions continues to grow throughout the entire axial compressive loading. At  $e=19.9\%$ , amorphous regions start to form at both tips of the SiNW as indicated by the non-dashed circles. At  $e=44.5\%$ , a sudden jump in amorphous atoms occurs due to zones of high tensile stresses at the zones indicated in Figure 9. The structure undergoes fracture at  $e=47.0\%$  due to rapid amorphization and a loss of crystalline structure induced by these tensile stresses.

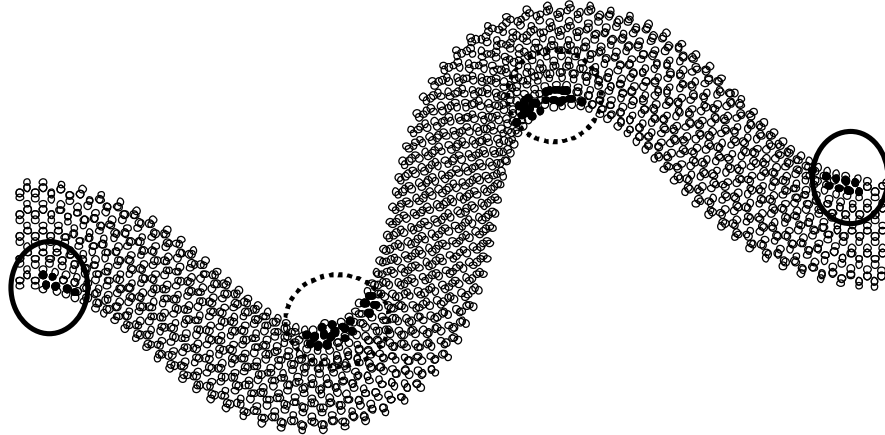


Figure 8. Cross sectional view of a SiNW under compression at 100000 timesteps ( $e=-29.9\%$ ). Zones of dense amorphous atoms are indicated by the circled region.

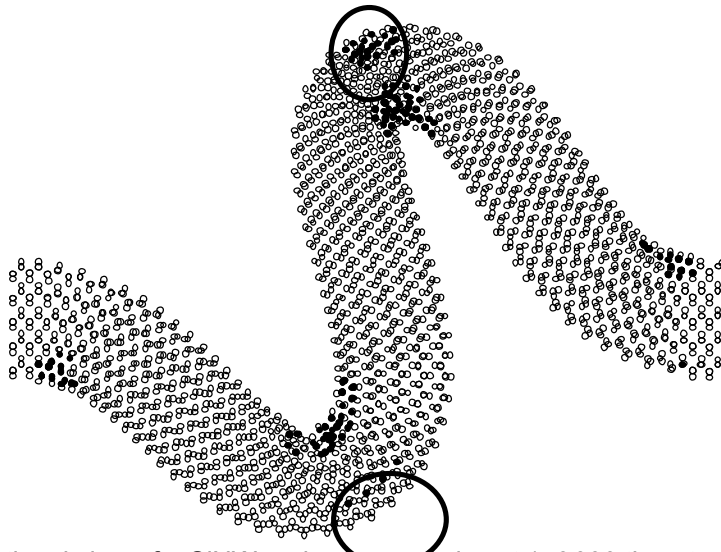


Figure 9. Cross sectional view of a SiNW under compression at 150000 timesteps just before fracture ( $e=-46.4\%$ ). Zones of dense amorphous atoms due to tensile stresses are indicated by the circled region.

Similar to the tensile simulation, the SiNW undergoes elastic deformation from  $e=0.0\%$  to  $e=-9.6\%$  with a proportional relationship between the stress and strain as shown in Figure 6. The critical buckling stress in this simulation is 34.0 GPa and the critical buckling force is  $1.46 \times 10^{-7}$  N. A comparison of this value with the theoretical continuum mechanics prediction would yield useful insights into the scale effect that occurs in buckling. The structure is treated as a column with both ends built-in and the critical buckling force is given by

$$P = \frac{4\pi^2 EI}{L^2} \quad (2)$$

where  $E$  is the Young's Modulus of elasticity and  $I$  is the second moment of area along the neutral axis.  $E$  is derived from the slope of the elastic region of the stress-strain graph and is calculated to be 351.90 GPa while the second moment of area is derived from assuming an elliptical geometrical cross-section of  $18818 \text{ \AA}^4$ . Using the formula above, the theoretical critical buckling force is  $2.88 \times 10^{-8}$  N. It is evident that there is a disagreement between the continuum mechanics prediction and the actual calculated value, primarily due to scale effects that arise from surface-surface interactions and a large surface area relative to volume [13].

## 4 Conclusions

An analysis of the microstructure and strain characteristics reveals that a SiNW exhibits gradual necking before the fracture point and rapid necking and formation of an atomic chain after the fracture point. The atomic chain unravels and does not break. In compression, the SiNW buckles at the critical buckling point and continues to undergo a crystalline-to-amorphous phase transformation in six distinct zones before the point of fracture, and that the strain-stress characteristics are consistent with the expectations of conventional continuum mechanics. A comparison between the actual and theoretical continuum mechanics prediction of the level of critical buckling stress indicates a poor agreement.

## References

- [1] Y. Cui, Z. Zhong, D. Wang, W. U. Wang & C. M. Lieber, Nano Letters 2003, Vol. 3, No. 2, pp. 149-152
- [2] S. W. Chung, J. Y. Yu, J. R. Heath, Applied Physics Letters 2000, Vol. 76, No. 15, pp. 2068-2070
- [3] D. Appell, Nature 2002, Vol. 419, pp. 553-555
- [4] Y. Cui, Q. Wei, H. Park, C. M. Lieber, Science 2001, Vol. 293, pp. 1289-1292
- [5] A. Hochbaum, R. Fan, R. He, P. Yang, Nano Letters 2005, Vol. 5, No. 3, pp. 457-460.
- [6] J. Kikkawa, Y. Ohno, S. Takeda, Applied Physics Letters 2005, Vol. 86, pp. 123109.
- [7] A. Mao, H. T. Ng, P. Nguyen, M. McNeil, M. Meyyappan, Journal of Nanoscience and Nanotechnology 2005, Vol. 5, No. 5, pp. 831-835
- [8] Y. L. Chueh, L. J. Chou, S. L. Cheng, J. H. He, W. W. Wu, L. J. Chen, Applied Physics Letters 2005, Vol. 86, pp. 133112
- [9] A. M. Morales & C. M. Lieber, Science 1998, Vol. 279, pp. 208-211
- [10] H. Üstunel, D. Roundy & T. A. Arias, Nano Letters 2005, Vol 5, pp. 523-526
- [11] M. Menon, D. Srivastava, I. Ponomareva, L. A. Chernozatonskii, Physical Review B 2004, Vol. 70, pp. 125313
- [12] C. S. Moura & L. Amaral, Nuclear Instrumentation and Methods in Physical Research B 2005, Vol. 228, pp. 37-4
- [13] S. Liu, C.S. Jayanthi, Z. Zhang, S.Y. Wu., Journal of Computational and Theoretical Nanoscience, Vol. 4 No. 2, pp. 275-281
- [14] J. Tersoff, Physical Review B 1989 Vol. 39 pp. 5566-5568
- [15] J. W.Kang, J. J. Seo, H. J. Hwang, <http://arxiv.org/ftp/cond-mat/papers/0210/0210038.pdf>
- [16] H. A. Wu, A. K. Soh, International Journal of Nonlinear Sciences and Numerical Simulation 2003, Vol. 4, pp. 233-238
- [17] J. J. Wortman, R. A. Evans, Journal Of Applied Physics, Vol. 36 No 1, pp. 153-156
- [18] H. Ikeda, Y. Qi, T. Cagin, K. Samwer, W. L. Johnson, W. A. Goddard III, Physical Review Letters 1999, Vol. 82, No. 14, pp. 2900-2903
- [19] T. X. Yu and L. C. Zhang, Plastic Bending: Theory and Applications, World Scientific 1996